Interstellar Dust

Jayant Murthy
Indian Institute of Astrophysics
jmurthy@yahoo.com
murthy@iiap.res.in
http://www.iiap.res.in

Interstellar Dust

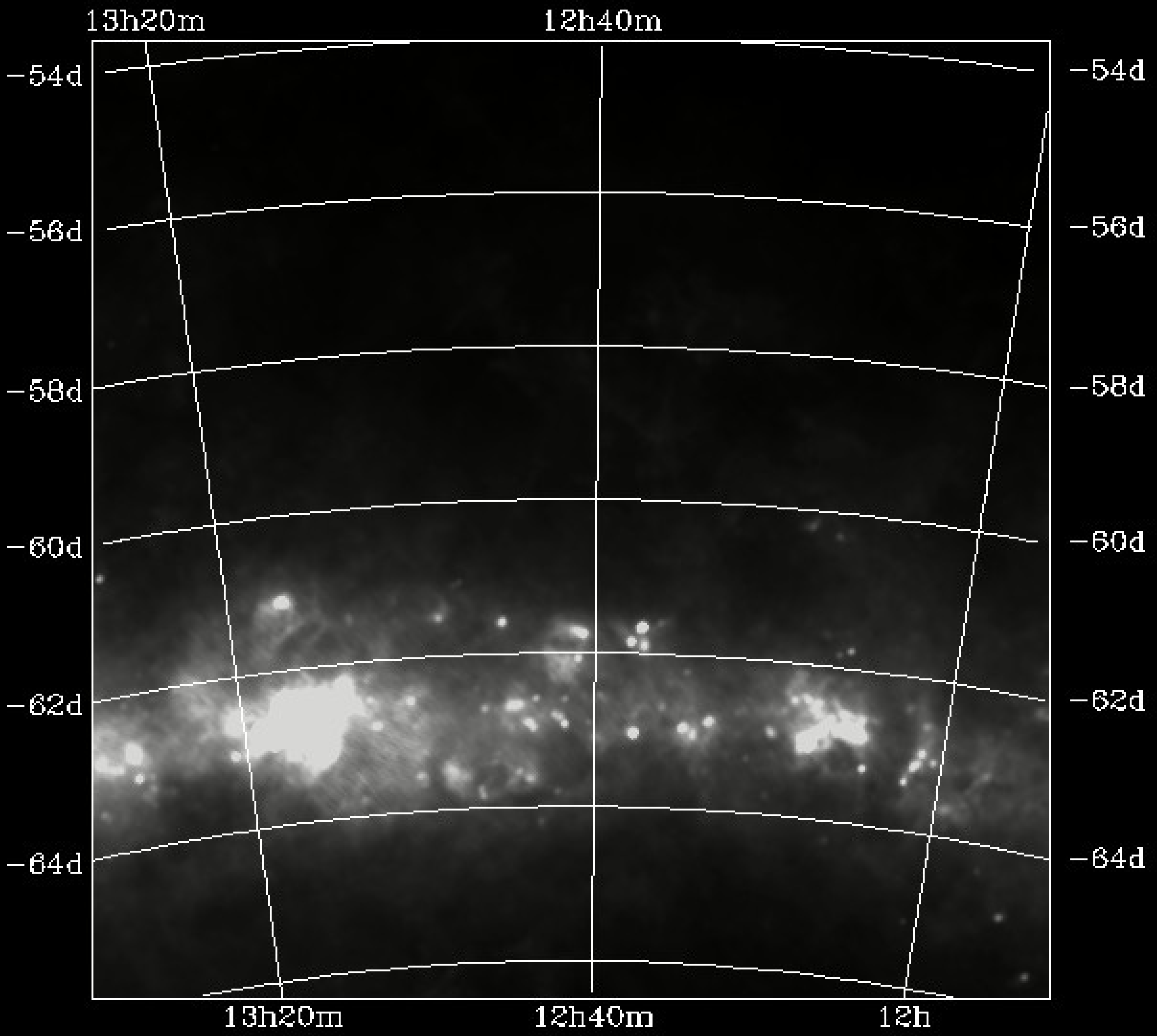

Dust Observations

- Extinction.
- Absorption.
- Scattering.
- $C_{ext} = C_{abs} + C_{sca}$
- $albedo = C_{sca}/C_{ext}$
- $< cos\theta >= \frac{1}{C_s ca} \int_0^\pi d\theta \frac{dC_s ca}{d\Omega} 2\pi sin\theta d\theta$

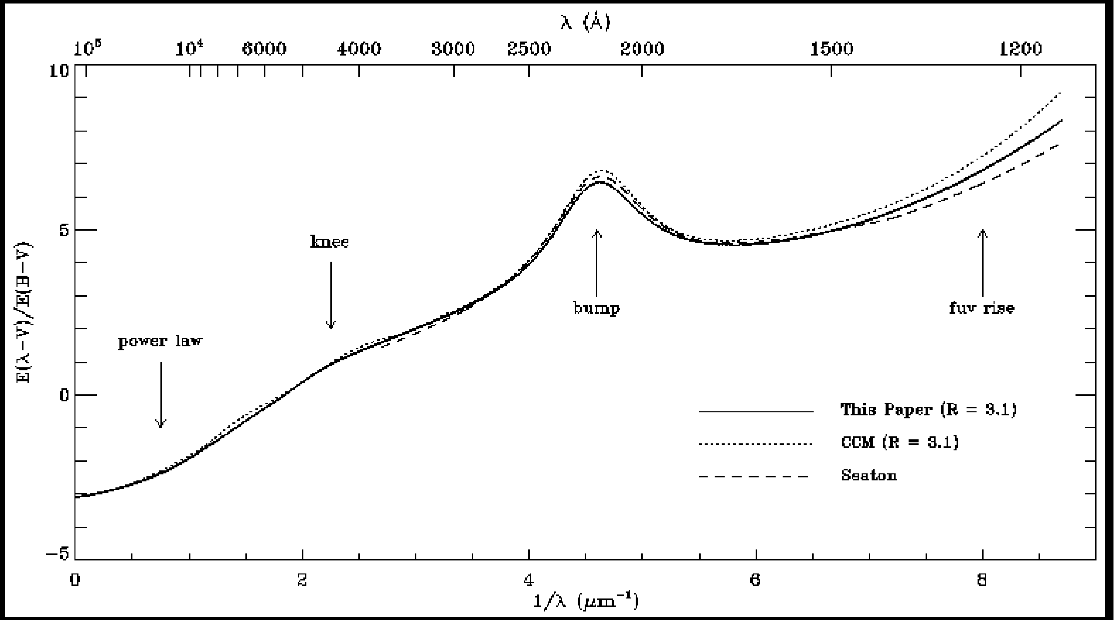

Dust Observations

- Extinction.
    - Absorption +
    - Scattering.
- Measure B and V.
- $E(B - V) = (B - V)_O - (B - V)_I$
    - $E(B - V) > 0$
- $A_\lambda = 2.5 \log(F_O - F_*) = 2.5\log(e^{-\tau}) = 1.086\tau$

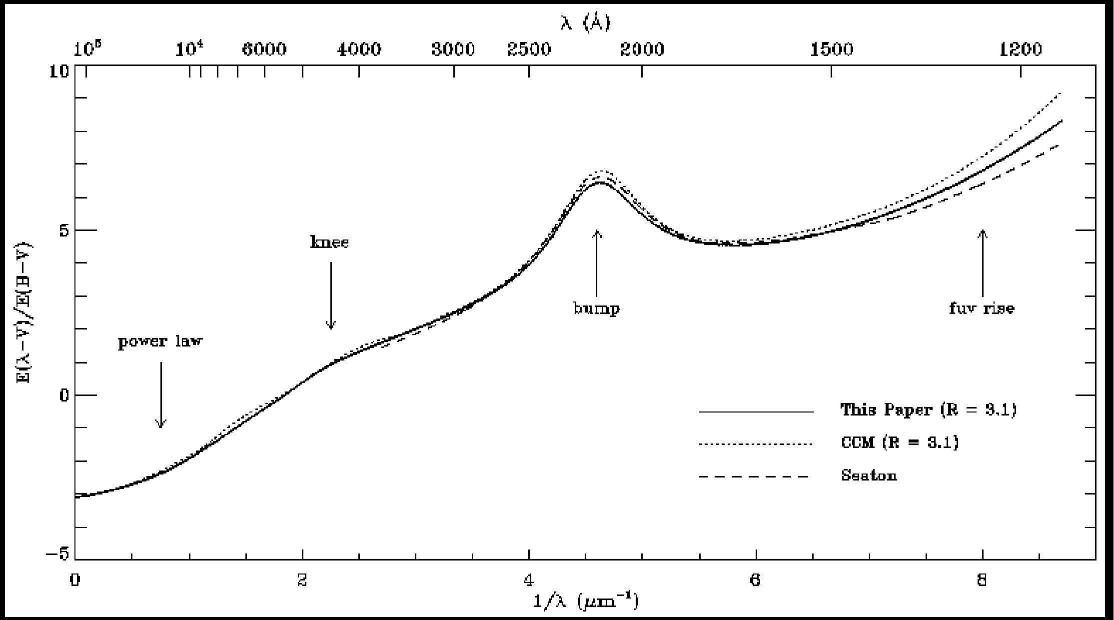

Dust Observations

- Extinction.
- Pair method
    - compare stars of similar spectral types.
    - use models instead of comparison stars.

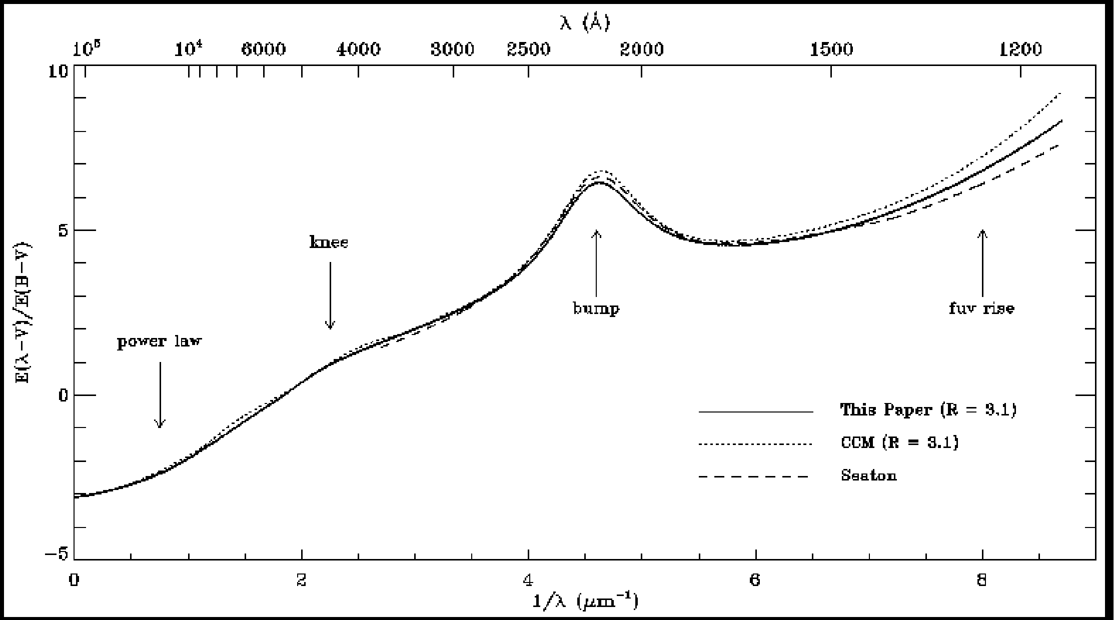

Dust Observations

- Extinction.
- Three populations:
  - Linear.
  - 2175 Å bump.
  - FUV rise.

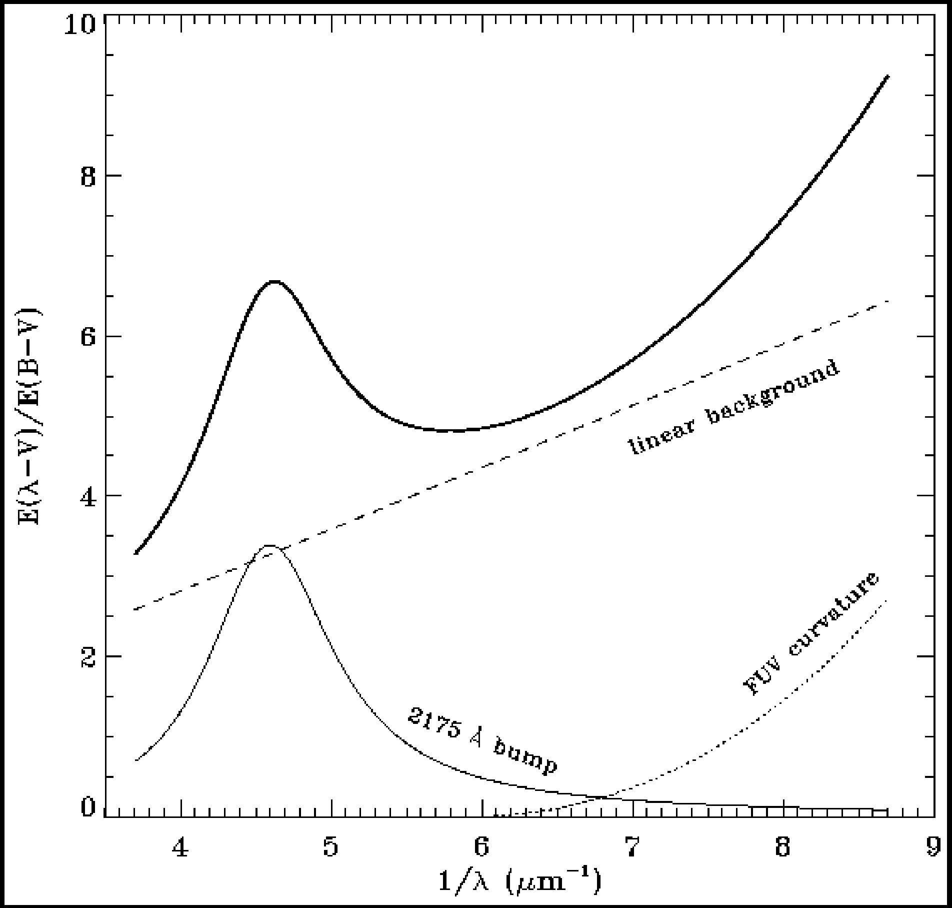

Dust Observations

- Extinction.
- Define

$$R_V \equiv A_V/(A_B - A_V)$$

- where A_V is the the extinction at V.
- $E(B - V) = A_B - A_V$

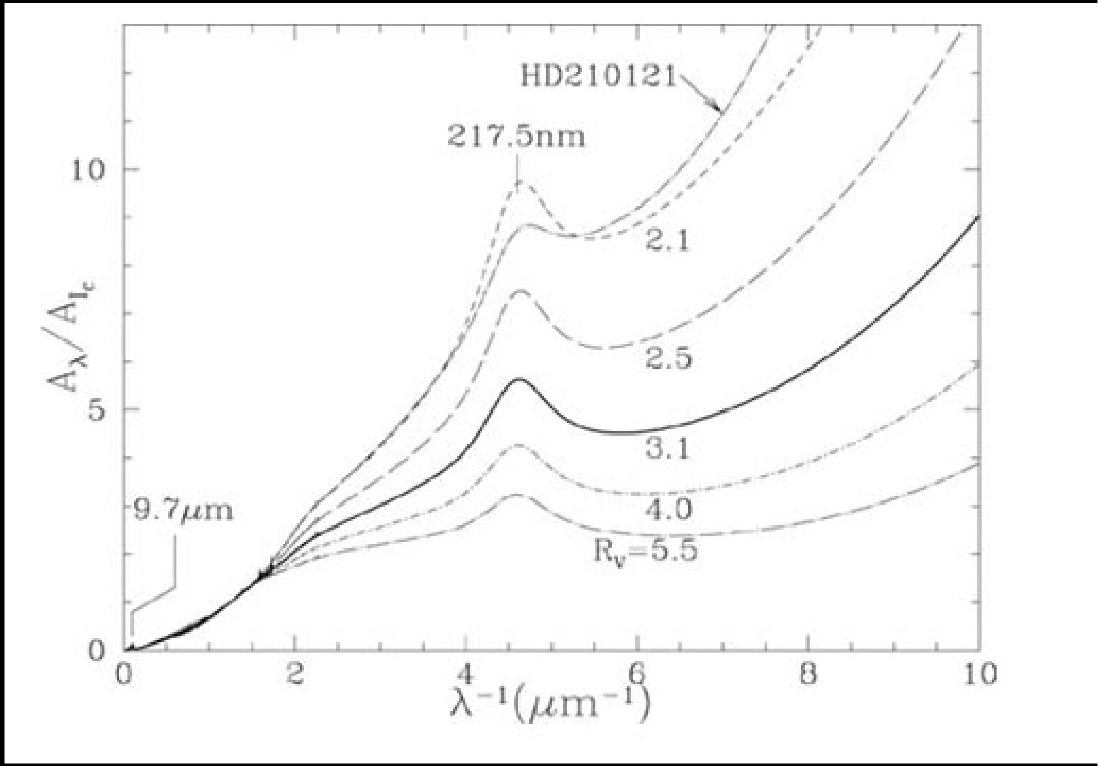

Dust Observations

- Extinction.
- Milky Way: R = 3.1
- Dense regions have larger R

Band	$\lambda(\mu m)$	A_λ/A_{I_C}	Band	$\lambda(\mu m)$	A_λ/A_{I_C}
M	4.75	0.0573	i	0.7480	1.125
L'	3.80	0.0842	R_C	0.6492	1.419
L	3.45	0.101	R_J	0.6415	1.442
K	2.19	0.212	r	0.6165	1.531
H	1.65	0.315	V	0.5470	1.805
J	1.22	0.489	g	0.4685	2.238
z	0.893	0.830	B	0.4405	2.396
I_J	0.8655	0.879	U	0.3635	2.813
I_C	0.8020	1.000	u	0.3550	2.867

Dust Observations

- Extinction.
- Parameterization of extinction curves
- Fitzgerald and Massa
- 7 parameter fit:
  - 3 bump
  - 3 UV extinction
  - 1 for long wavelength law.

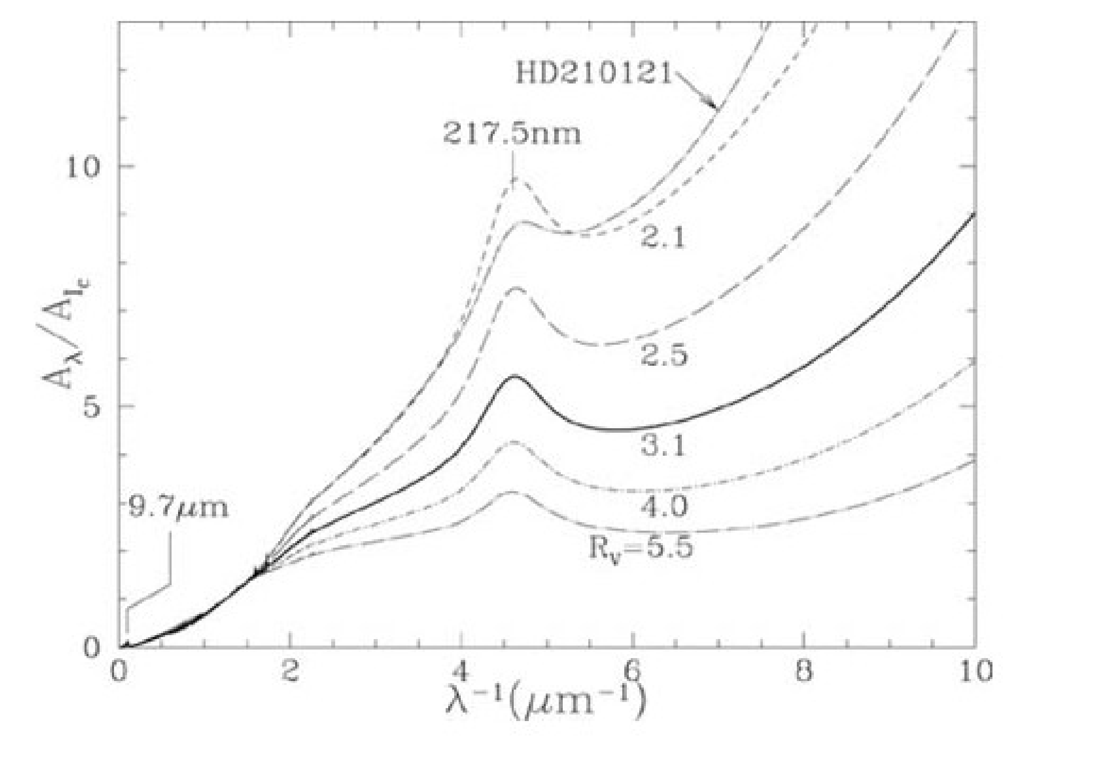

Dust Observations

- Extinction.
- Parameterization of extinction curves
- CCM:

We have fitted the families of extinction laws as functions of x ($\equiv 1/\lambda$) and ($1/R$) with analytical formulae similar to the expressions of FM86. We find the following interpolation formula, which gives good fits for 3.3 $\mu\mathrm{m}^{-1} < x < 8$ $\mu\mathrm{m}^{-1}$ and $2.5 < R < 6.5$:

$$\langle A(\lambda)/A(V) \rangle = a(x) + b(x)/R \; ; \tag{1}$$

where

$$a(x) = 1.802 - 0.316x - 0.104/[(x - 4.67)^2 + 0.341] + F_a(x) \; ;$$

$$b(x) = -3.090 + 1.825x + 1.206/[(x - 4.62)^2 + 0.263] + F_b(x) \; ;$$

$$F_a(x) = -0.04473(x - 5.9)^2 - 0.009779(x - 5.9)^3 \, , \; (x \geq 5.9) \; ;$$

$$F_b(x) = 0.2130(x - 5.9)^2 + 0.1207(x - 5.9)^3 \, , \; (x \geq 5.9) \; ;$$

and

$$F_a(x) = F_b(x) = 0 \, , \; (x < 5.9) \, .$$

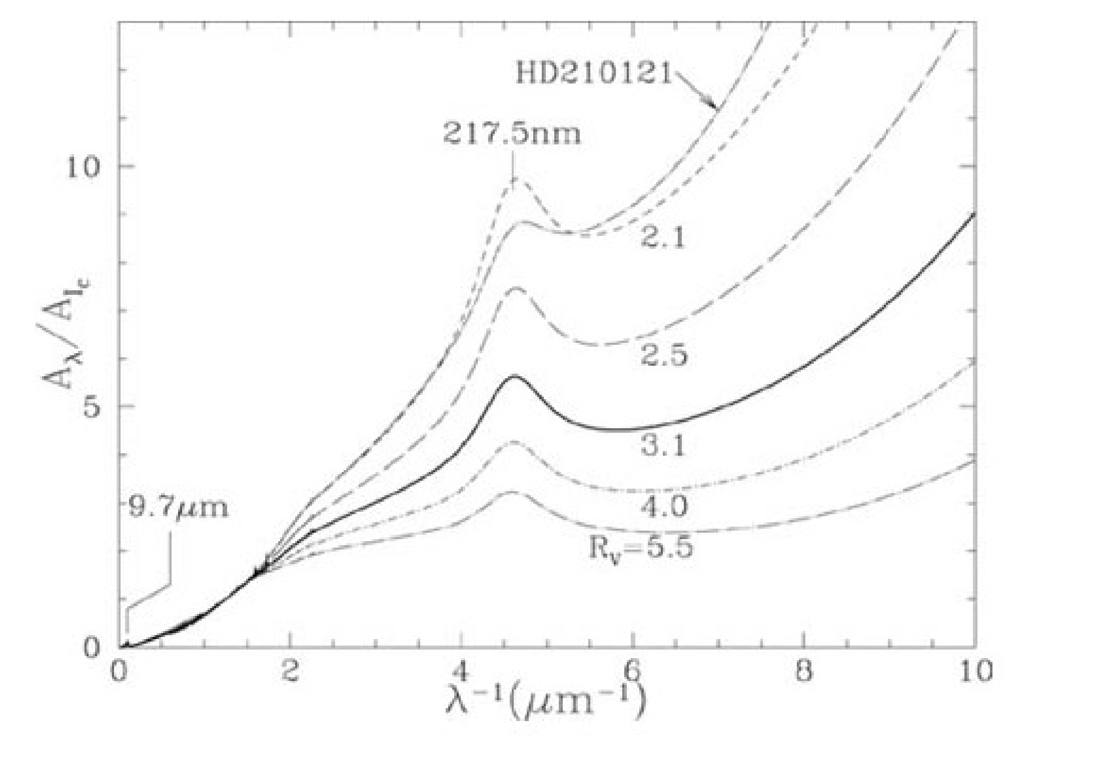

Dust Observations

- Extinction.
- Long wavelength cutoff at 1 μm
  - implies largest grains ~ 1 μm in size.
  - 2175 Å due to graphitic particles.
  - FUV rise due to population of small particles.

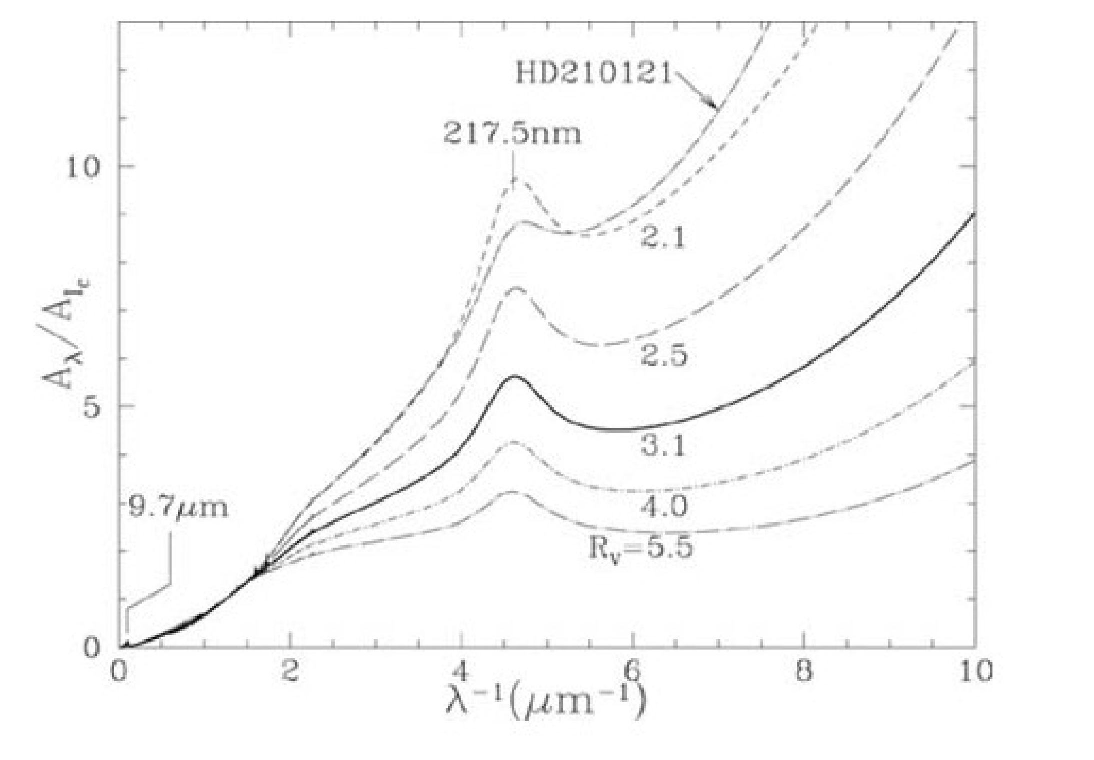

Dust Observations

- Extinction.
- Dust and gas well mixed.
- Bohlin, Savage, Dr
- N(H) = 5.8e21E(B

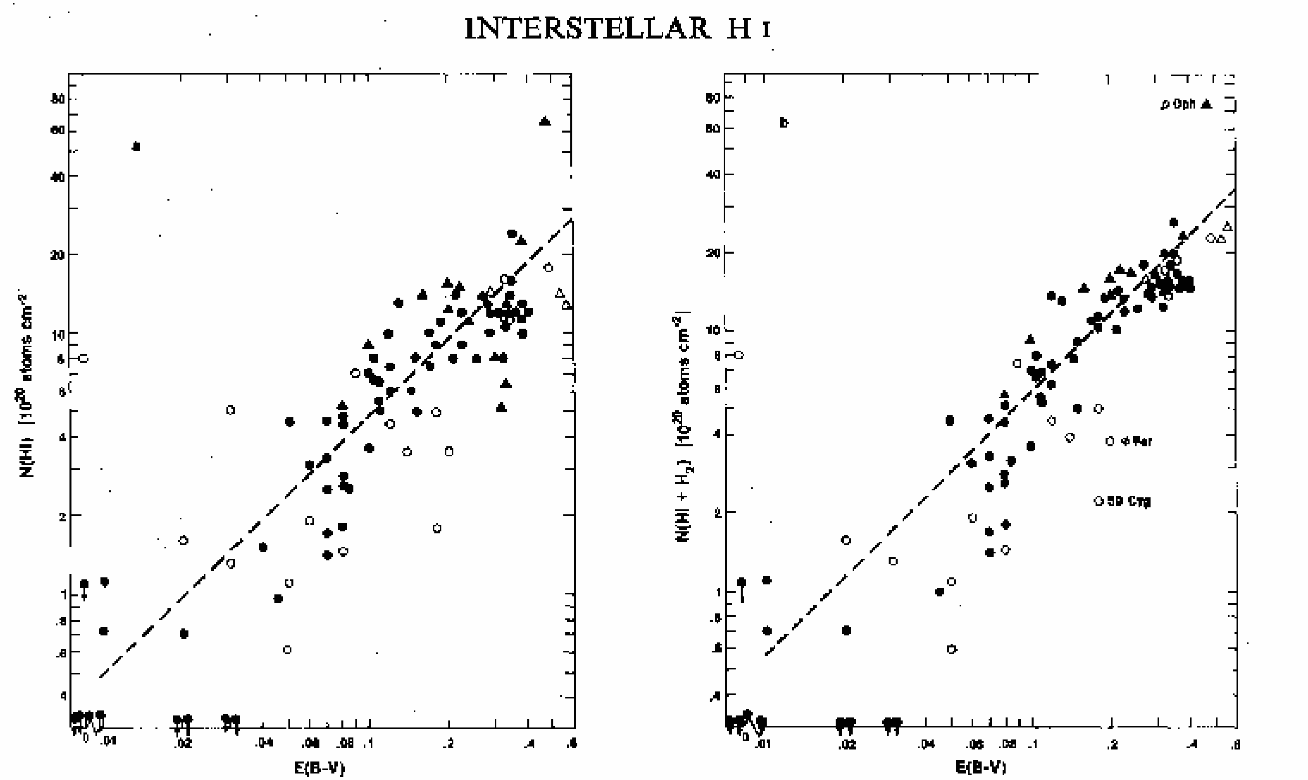

) The correlation between the atomic hydrogen column density N(H I) and $E(B-V)$. (b) The correlation
rogen column density, $N(\text{H I} + H_2) = N(\text{H I}) + 2N(H_2)$, and $E(B-V)$. In both (a) and (b), the dashed
atios from Table 2. *Triangles*, stars with high mean densities, $n(\text{H I} + H_2) > 1$ atom cm^{-3}; *circles*, cas
< 1 atom cm^{-3}. *Open symbols*, stars with uncertain $E(B-V)$ that were omitted in calculating the mean rat

Dust Observations

- Extinction.
- Polarization
- Dust grains aligned with magnetic field.

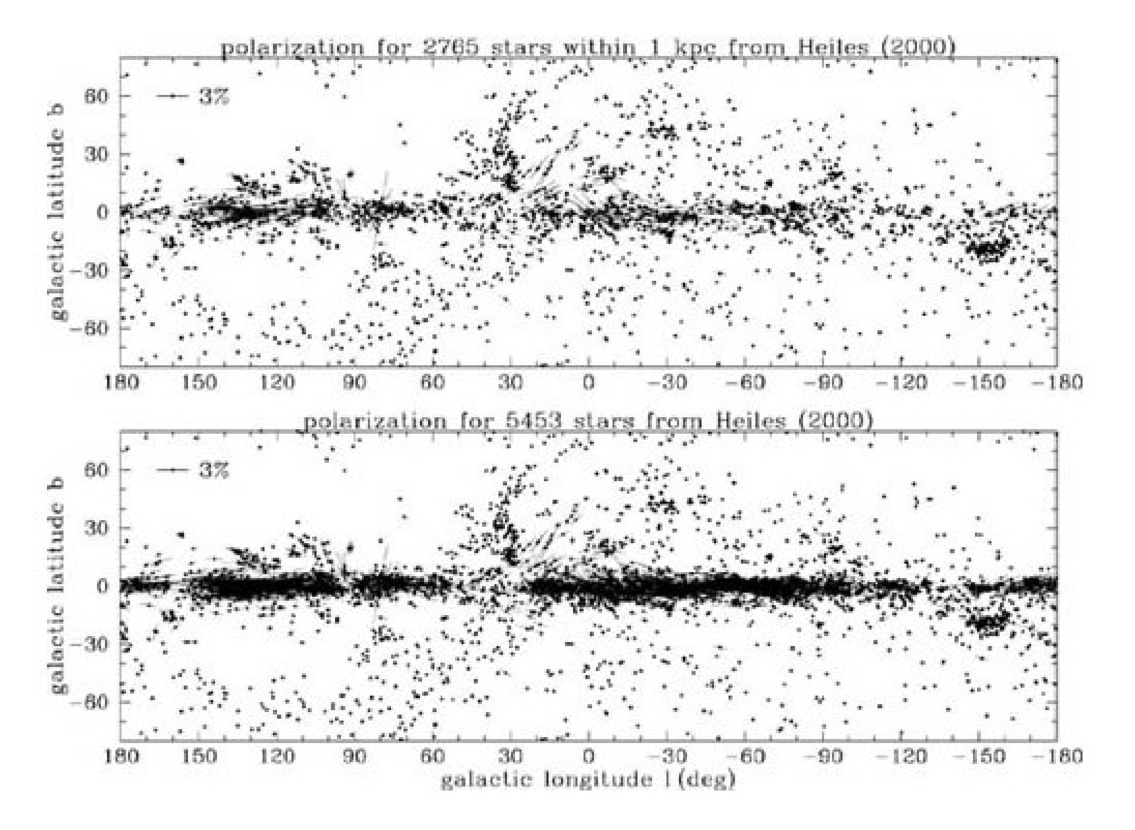

Dust Observations

- Extinction.
- Polarization
- Serkowski Law:
- $p(\lambda) = p_{max} \exp(-K \ln^2(\lambda/\lambda_{max}))$
  - $\lambda_{max} = 5500$ Å
  - $K = 1.15$
- $0 < p_{max} < 0.03\ A_V$

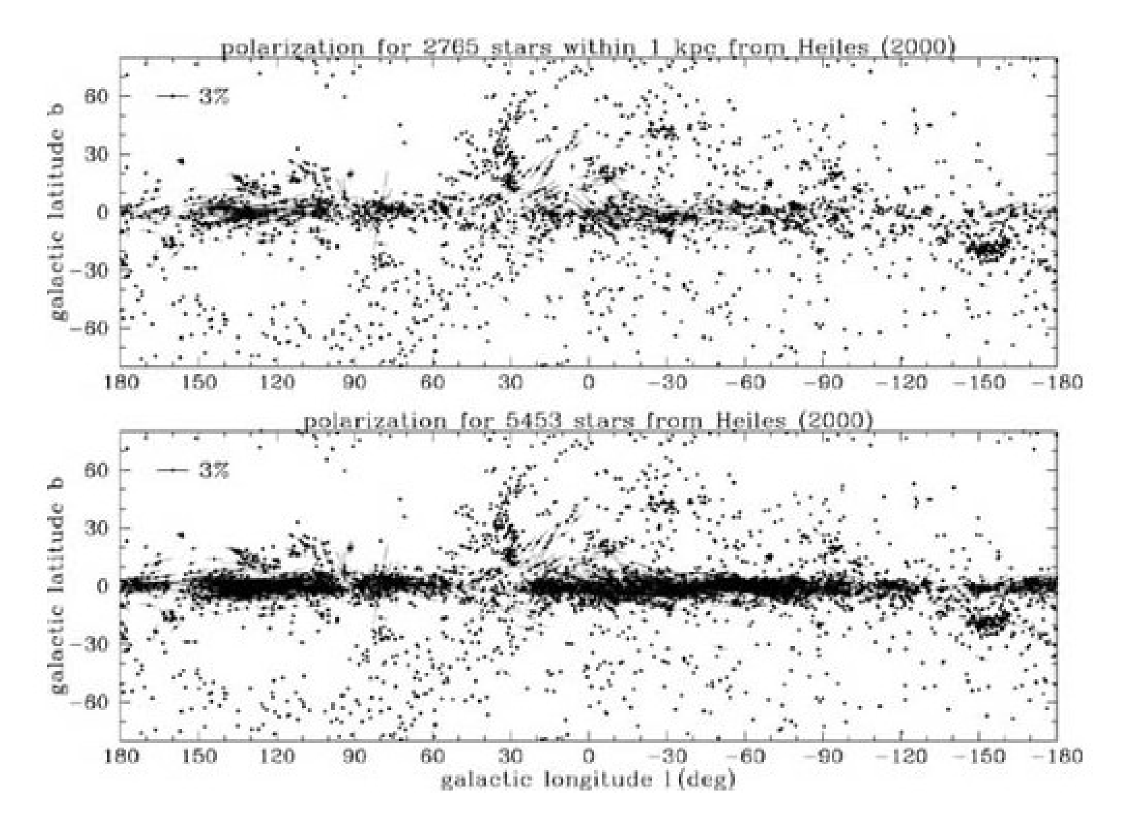

Dust Observations

- Extinction.
- Polarization
- Due to grains with shortest axes partially aligned with magnetic field.
- Largest values where magnetic field perpendicular with line of sight.

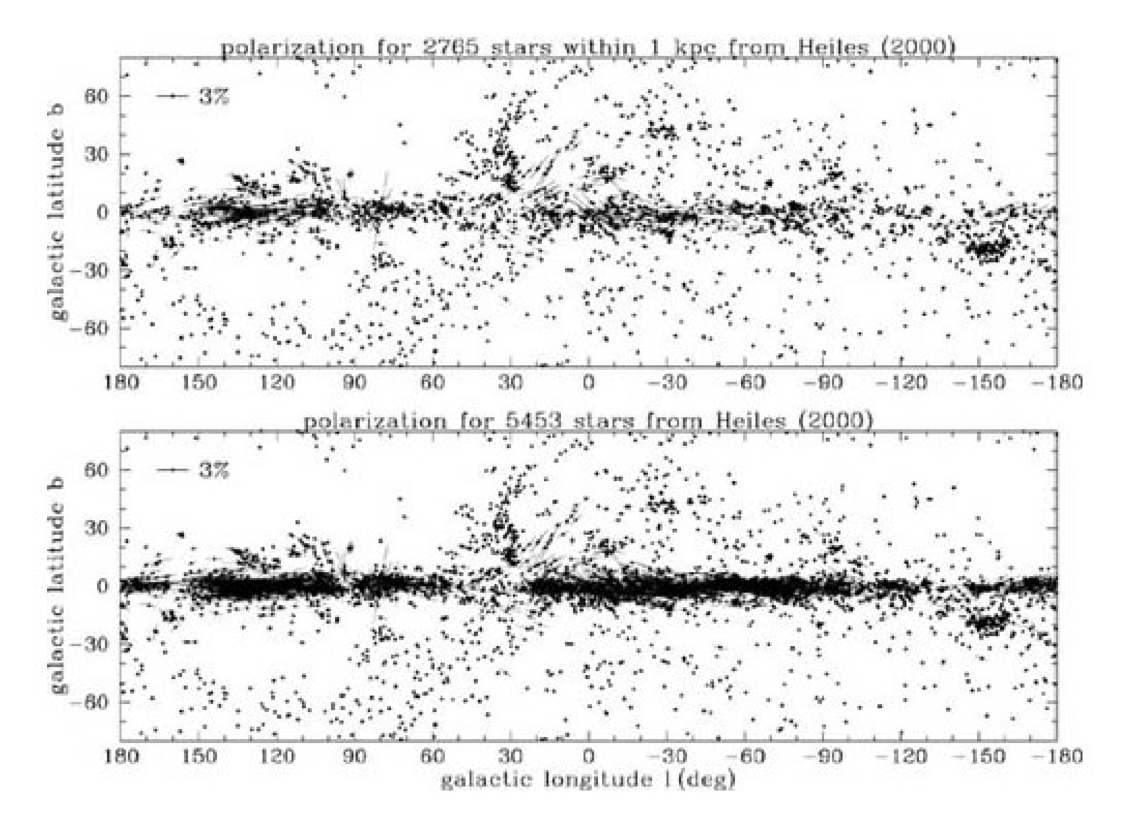

Dust Observations

- Extinction.
- Polarization
- Decreases to UV suggesting that particle sizes approach geometrical optics limit

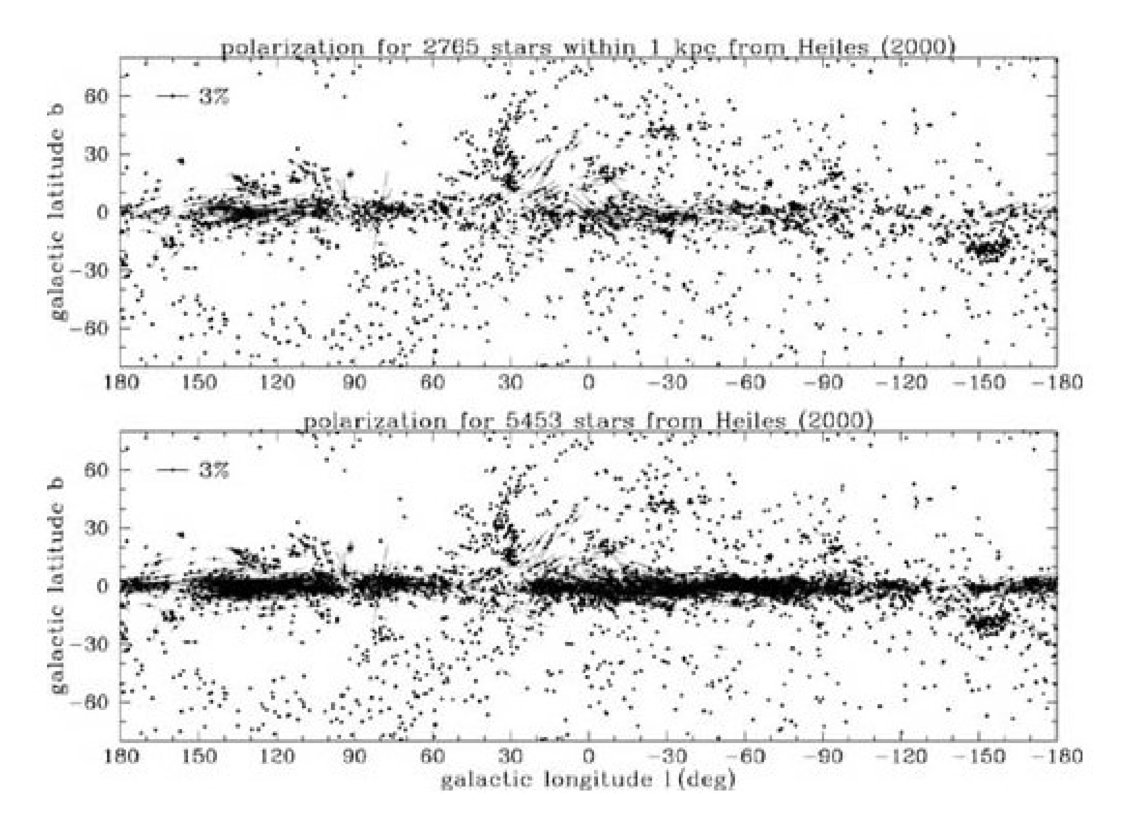

Dust Observations

- Extinction.
- Polarization
- Dust scattering.
- Reflection nebulae.
- Diffuse background light.

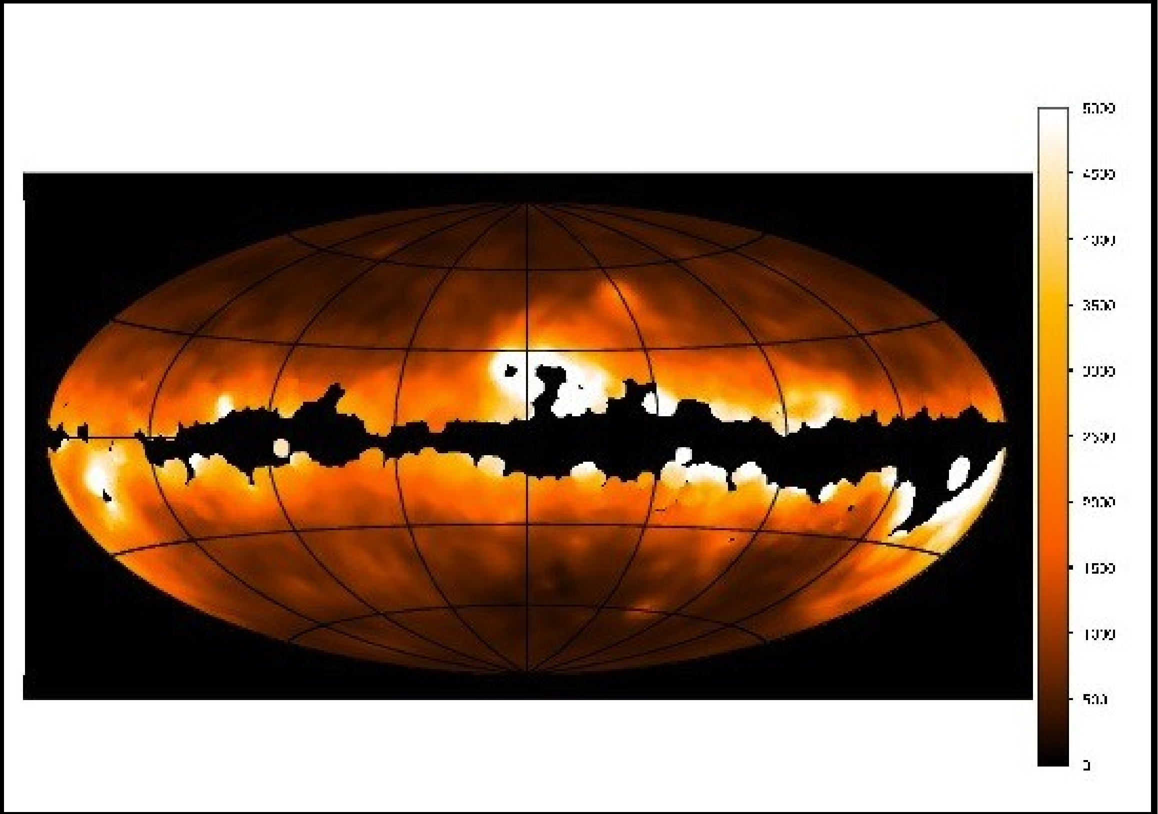

Dust Observations

- Extinction.
- Polarization
- Dust scattering.
  - Reflection nebulae.
  - Diffuse background light.
- Measure *a* and *g* = <cosθ>

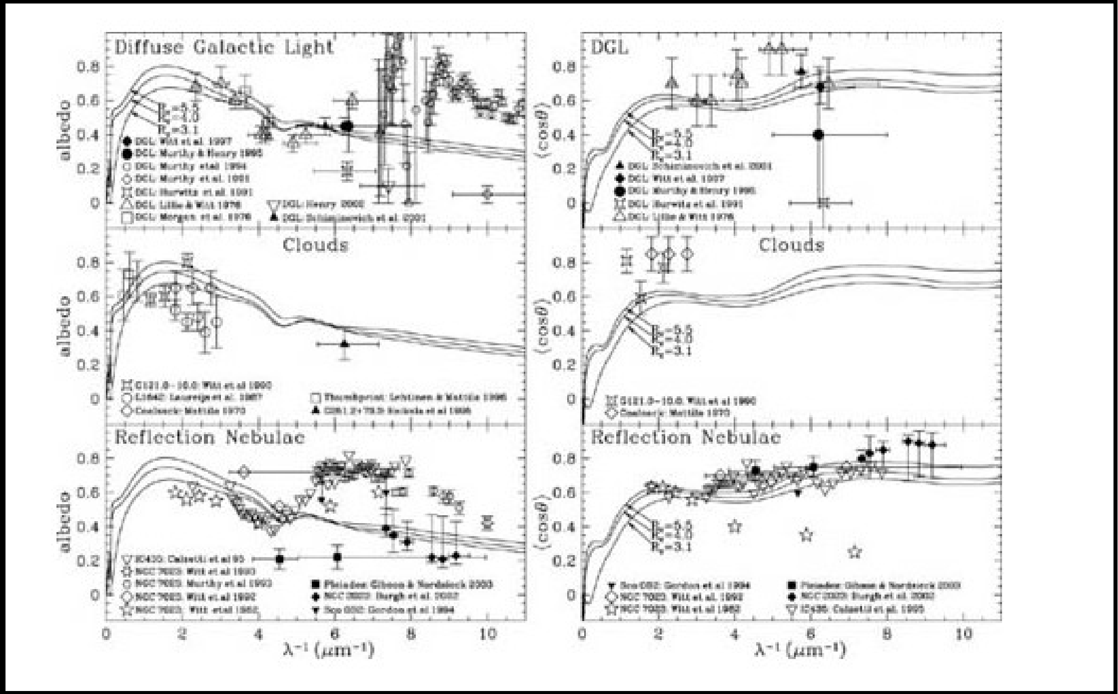

Dust Observations

- Extinction.
- Polarization
- Dust scattering.
    - Reflection nebulae.
    - Diffuse background light.
- Measure *a* and $g = \langle\cos\theta\rangle$

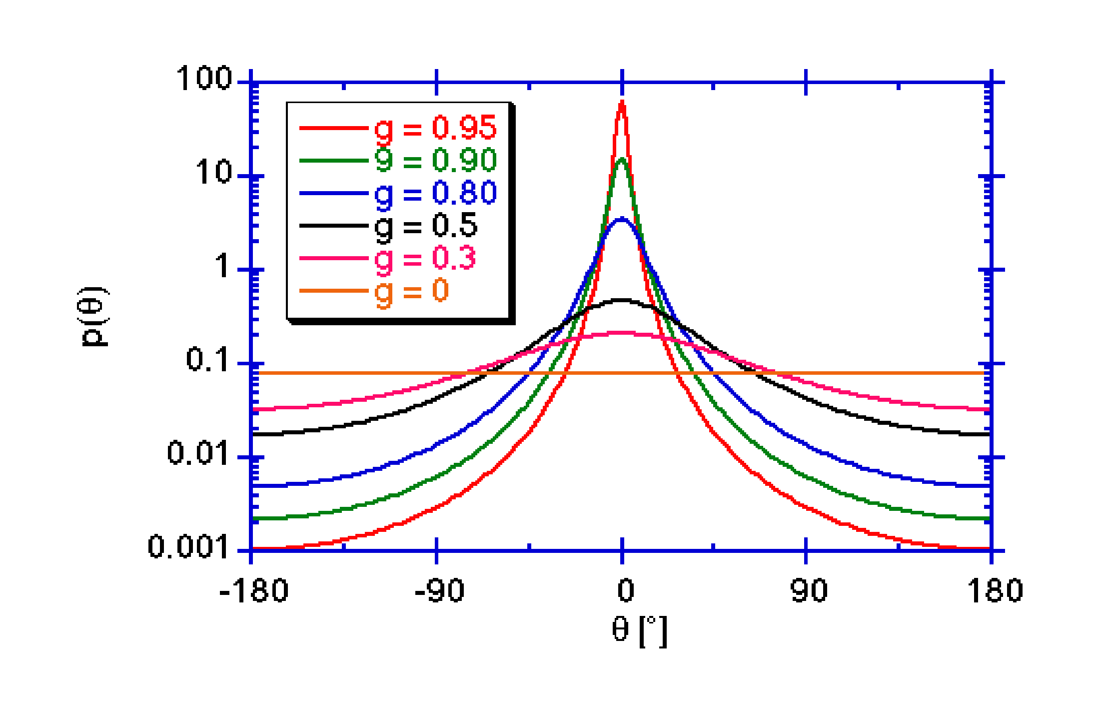

Dust Observations

- Extinction.
- Polarization
- Dust scattering.
- Thermal emission.
    - Zodiacal light.
    - Galactic light.

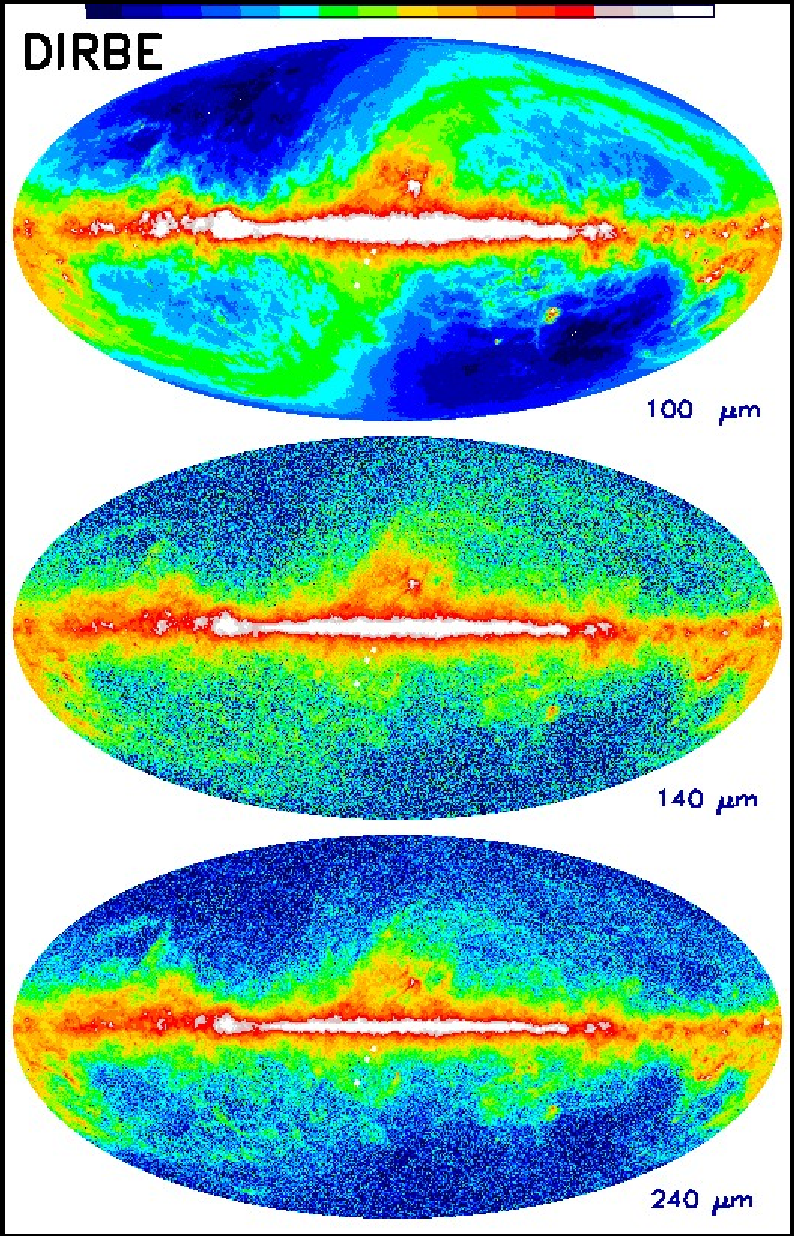

Dust Observations

- Extinction.
- Polarization
- Dust scattering.
- Thermal emission.
    - Blackbody at long wavelengths.
    - Stochastic at short wavelengths.
    - Line emission.

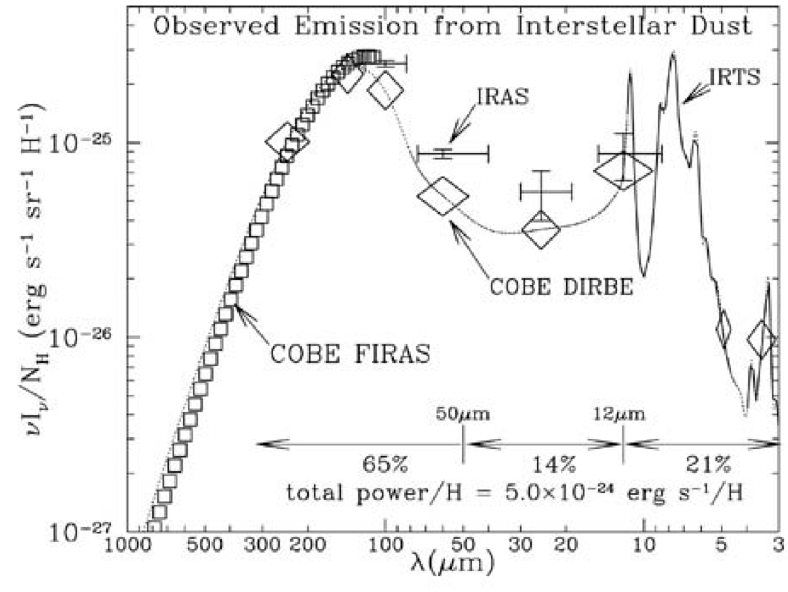

Figure 21.6 Observed infrared emission per H nucleon from dust heated by the average starlight background in the local Milky Way. Crosses: IRAS (Boulanger & Perault 1988); squares: COBE-FIRAS (Wright et al. 1991); diamonds: COBE-DIRBE (Arendt et al. 1998); heavy curve: IRTS (Onaka et al. 1996; Tanaka et al. 1996). The interpolated dotted line is used to estimate the total power.

Dust Observations

- Extinction.
- Polarization
- Dust scattering.
- Thermal emission.
- ERE.
- Small angle X-ray scattering.
- Microwave emission from spinning ultra-small grains.

Proto-Planetary Nebula ▪ Red Rectangle ▪ HD 44179 *HST* ▪ WFPC2

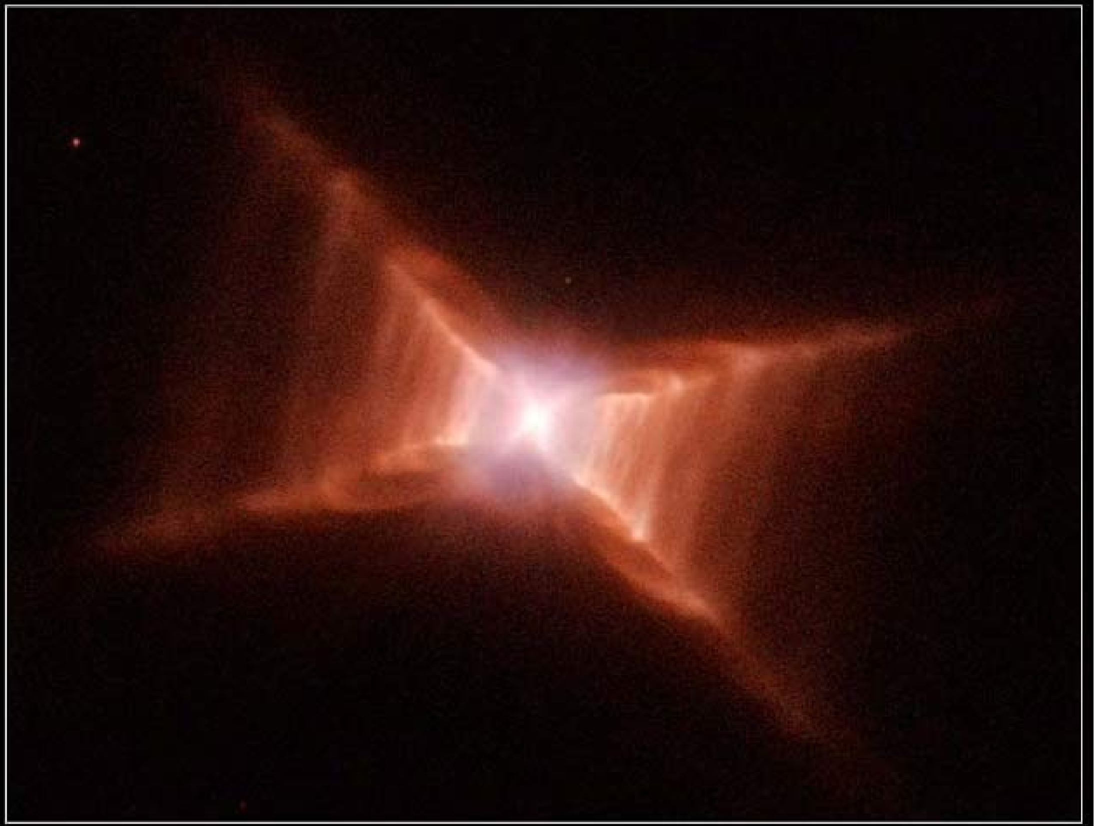

NASA, ESA, H. Van Winckel (Catholic University of Leuven) and M. Cohen (University of California, Berkeley) STScI-PRC04-11

Dust Composition

- From Kramers-Kronig relation and extinction curve:
    - $M_{dust}/M_H > 0.0083$
- Implies that dust must be comprised of C, O, Mg, Si, S, Fe.

Element	Solar[a]	WIM $F_* = -0.1$	WNM $F_* = 0.1$	CNM $F_* = 0.4$	Diffuse H_2 $F_* = 0.8$
C[b]	295.	114.	111.	109.	93.
N	74.	62.	62.	62.	62.
O	537.	592.	534.	457.	372.
Na	2.04	(2.)	(2.)	(2.)	(2.)
Mg	43.7	28.1	17.8	8.9	3.6
Al	2.95	(0.54)	(0.27)	(0.097)	(0.025)
Si	35.5	31.6	18.7	8.5	3.0
S	14.5	14.5	14.5	11.8	5.3
Ca	2.14	(0.39)	(0.20)	(0.070)	(0.018)
Ti	0.089	0.013	0.0052	0.0013	0.0002
Fe	34.7	5.2	2.9	1.19	0.36
Ni	1.74	0.32	0.16	0.057	0.015
M^{+} [c]	432.	197.	168.	142.	107.

[a] From Table 1.4.
[b] Gas-phase C abundance from Jenkins (2009) reduced by factor 2 (see text).
[c] Photoionizable "metals": $M = C + Na + Mg + Si + S + Fe + 3.9 \times Ni$.

Dust Composition

- From Kramers-Kronig relation and extinction curve:
  - $M_{dust}/M_H > 0.0083$
- Implies that dust must be comprised of C, O, Mg, Si, S, Fe.

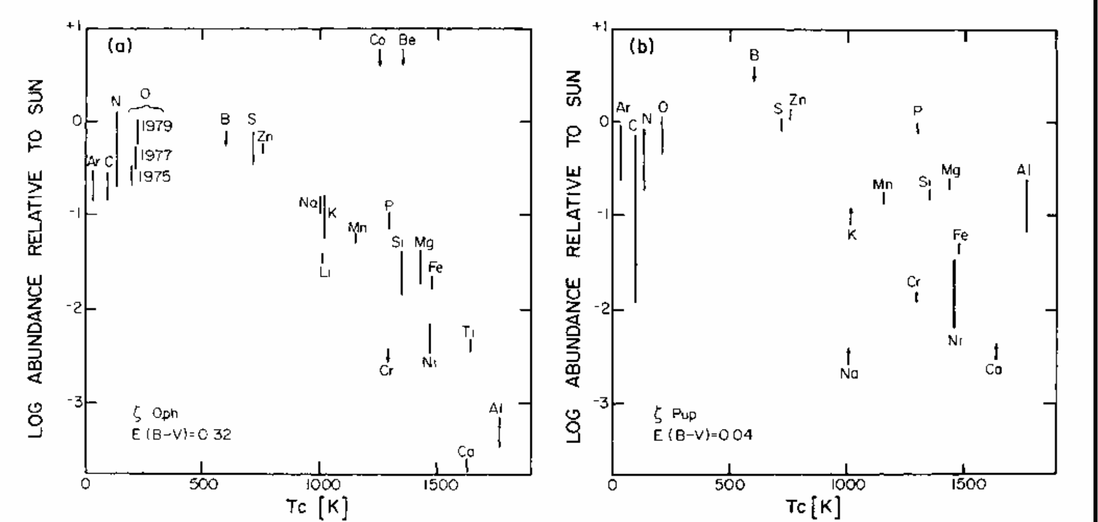

Figure 3 Elemental depletion is plotted versus condensation temperature for a moderately reddened line of sight in (*a*) and a lightly reddened line of sight in (*b*). The data are from Morton (1975) for ζ Oph in (*a*) and Morton (1978) for ζ Pup in (*b*). These results have been supplemented by more recent estimates

Dust Composition

- 28% of dust mass in C.
- 72% in other compounds.
    - silicates.
- Oxygen problem.
    - Missing in some sightlines.
    - Too much in other sightlines.

Table 23.1 Inferred Elemental Composition of Dust toward ζ Oph

X	$(N_X/N_{\rm H})_\odot$ [a] (ppm)	$N_{X,\rm gas}/N_{\rm H}$ [b] (ppm)	$N_{X,\rm dust}/N_{\rm H}$ (ppm)	$10^3 M_{X,\rm dust}/M_{\rm H}$
C	295 ± 36	135 ± 33 [d,e]	160 ± 49	1.92 ± 0.59 [e]
		85 ± 20 [d,f]	210 ± 41	2.52 ± 0.49 [f]
N	74.1 ± 9.0	78 ± 13 [g]	-14 ± 16	0
O	537 ± 62	295 ± 36 [d]	242 ± 72	3.87 ± 1.15
		[383] [c]	154 ± 8 [c]	2.46 ± 0.13 [c]
Mg	43.7 ± 4.2	4.9 ± 0.5 [g]	39 ± 4	0.94 ± 0.10
Al	2.8 ± 0.2	0.005 ± 0.001 [h]	2.8 ± 0.2	0.08 ± 0.01
Si	35.5 ± 3.0	1.7 ± 0.5 [i]	34 ± 3	0.95 ± 0.08
S	14.5 ± 1.0	28 ± 16 [j]	-14 ± 16	0
Ca	2.3 ± 0.2	0.0004 ± 0.0001 [k]	2.2 ± 0.2	0.09 ± 0.008
Fe	34.7 ± 3.3	0.13 ± 0.01 [g]	35 ± 3	1.96 ± 0.17
Ni	1.7 ± 0.2	0.0030 ± 0.0002 [j]	1.7 ± 0.2	0.10 ± 0.01
Total if $f(\text{C II}]2325) = 4.78 \times 10^{-8}$ (see text)				9.9 ± 1.3 [e]
Total if $f(\text{C II}]2325) = 1.0 \times 10^{-7}$ (see text)				10.5 ± 1.3 [f]
Total if $f(\text{C II}]2325) = 1.0 \times 10^{-7}$, $N_{\rm O,dust}/N_{\rm H} = 154$ ppm (see text)				9.1 ± 0.6 [c]

[a] Asplund et al. (2009).
[b] Assuming $N(\rm H)+2N(\rm H_2)=10^{21.13\pm0.03}$ cm^{-2}.
[c] Assuming $N_{\rm O,dust}/N_{\rm H} = 154$ ppm.
[d] Cardelli et al. (1993).
[e] If $f(\text{C II}]2325\,\text{Å}) = 4.78 \times 10^{-8}$ (Morton 2003).
[f] If $f(\text{C II}]2325\,\text{Å}) = 1.00 \times 10^{-7}$ (see text).
[g] Savage et al. (1992).
[h] Morton (1975).
[i] Cardelli et al. (1994).
[j] Federman et al. (1993).
[k] Crinklaw et al. (1994).

Dust Composition

- Meteoritic composition.
    - Presolar grains.
- Selection effects in identification of grains and their survival.

Material	Source	Grain Size (μm)	Abundance[c] (ppm)†
Amorphous silicates	Circumstellar	0.2–0.5	20–3600
Forsterite (Mg_2SiO_4) } Enstatite ($MgSiO_3$)	Circumstellar	0.2–0.5	10–1800
Diamond		$\sim$0.002	$\sim$1400
P3 fraction	Not known		
HL fraction	Circumstellar		
Silicon carbide	Circumstellar	0.1–20	13–14
Graphite	Circumstellar	0.1–10	7–10
Spinel ($MgAl_2O_4$)	Circumstellar	0.1–3	1.2
Corundum (Al_2O_3)	Circumstellar	0.5–3	0.01
Hibonite ($CaAl_{12}O_{19}$)	Circumstellar	1–2	0.02

[a] Other presolar materials include TiC, MoC, ZrC, RuC, FeC, Si_3N_4, TiO_2, and Fe-Ni metal.

[b] See Huss & Draine (2007) for details and references therein.

[c] Abundance in fine-grained fraction (= matrix in primitive chondrites).

Dust Composition

- Silicates
  - pyroxene
  - olivine
- Oxides
  - Silicon
  - Iron
  - Mg

Table 23.1 Inferred Elemental Composition of Dust toward ζ Oph

X	$(N_X/N_{\rm H})_\odot$ [a] (ppm)	$N_{X,\rm gas}/N_{\rm H}$ [b] (ppm)	$N_{X,\rm dust}/N_{\rm H}$ (ppm)	$10^3 M_{X,\rm dust}/M_{\rm H}$
C	295 ± 36	135 ± 33 [d,e]	160 ± 49	1.92 ± 0.59 [e]
		85 ± 20 [d,f]	210 ± 41	2.52 ± 0.49 [f]
N	74.1 ± 9.0	78 ± 13 [g]	-14 ± 16	0
O	537 ± 62	295 ± 36 [d]	242 ± 72	3.87 ± 1.15
		[383] [c]	154 ± 8 [c]	2.46 ± 0.13 [c]
Mg	43.7 ± 4.2	4.9 ± 0.5 [g]	39 ± 4	0.94 ± 0.10
Al	2.8 ± 0.2	0.005 ± 0.001 [h]	2.8 ± 0.2	0.08 ± 0.01
Si	35.5 ± 3.0	1.7 ± 0.5 [i]	34 ± 3	0.95 ± 0.08
S	14.5 ± 1.0	28 ± 16 [j]	-14 ± 16	0
Ca	2.3 ± 0.2	0.0004 ± 0.0001 [k]	2.2 ± 0.2	0.09 ± 0.008
Fe	34.7 ± 3.3	0.13 ± 0.01 [g]	35 ± 3	1.96 ± 0.17
Ni	1.7 ± 0.2	0.0030 ± 0.0002 [j]	1.7 ± 0.2	0.10 ± 0.01
Total if $f(\text{C II]}2325) = 4.78 \times 10^{-8}$ (see text)				9.9 ± 1.3 [e]
Total if $f(\text{C II]}2325) = 1.0 \times 10^{-7}$ (see text)				10.5 ± 1.3 [f]
Total if $f(\text{C II]}2325) = 1.0 \times 10^{-7}$, $N_{\rm O,dust}/N_{\rm H} = 154$ ppm (see text)				9.1 ± 0.6 [c]

[a] Asplund et al. (2009).
[b] Assuming $N(\mathrm{H})+2N(\mathrm{H_2})=10^{21.13\pm0.03}\ \mathrm{cm^{-2}}$.
[c] Assuming $N_{\rm O,dust}/N_{\rm H} = 154$ ppm.
[d] Cardelli et al. (1993).
[e] If $f(\text{C II]}2325\ \text{Å}) = 4.78 \times 10^{-8}$ (Morton 2003).
[f] If $f(\text{C II]}2325\ \text{Å}) = 1.00 \times 10^{-7}$ (see text).
[g] Savage et al. (1992).
[h] Morton (1975).
[i] Cardelli et al. (1994).
[j] Federman et al. (1993).
[k] Crinklaw et al. (1994).

Dust Composition

- Solid carbon
  - Graphite.
  - Diamond.
  - Amorphous.
  - Nanoparticles.
- Hydrocarbons
  - PAHs
  - HACs
- Fe.
- Silicon carbide.

Table 23.1 Inferred Elemental Composition of Dust toward ζ Oph

X	$(N_X/N_{\rm H})_\odot$ [a] (ppm)	$N_{X,\rm gas}/N_{\rm H}$ [b] (ppm)	$N_{X,\rm dust}/N_{\rm H}$ (ppm)	$10^3 M_{X,\rm dust}/M_{\rm H}$
C	295 ± 36	135 ± 33 [d,e]	160 ± 49	1.92 ± 0.59 [e]
		85 ± 20 [d,f]	210 ± 41	2.52 ± 0.49 [f]
N	74.1 ± 9.0	78 ± 13 [g]	-14 ± 16	0
O	537 ± 62	295 ± 36 [d]	242 ± 72	3.87 ± 1.15
		[383] [c]	154 ± 8 [c]	2.46 ± 0.13 [c]
Mg	43.7 ± 4.2	4.9 ± 0.5 [g]	39 ± 4	0.94 ± 0.10
Al	2.8 ± 0.2	0.005 ± 0.001 [h]	2.8 ± 0.2	0.08 ± 0.01
Si	35.5 ± 3.0	1.7 ± 0.5 [i]	34 ± 3	0.95 ± 0.08
S	14.5 ± 1.0	28 ± 16 [j]	-14 ± 16	0
Ca	2.3 ± 0.2	0.0004 ± 0.0001 [k]	2.2 ± 0.2	0.09 ± 0.008
Fe	34.7 ± 3.3	0.13 ± 0.01 [g]	35 ± 3	1.96 ± 0.17
Ni	1.7 ± 0.2	0.0030 ± 0.0002 [j]	1.7 ± 0.2	0.10 ± 0.01
Total if $f(\text{C II]}2325) = 4.78 \times 10^{-8}$ (see text)				9.9 ± 1.3 [e]
Total if $f(\text{C II]}2325) = 1.0 \times 10^{-7}$ (see text)				10.5 ± 1.3 [f]
Total if $f(\text{C II]}2325) = 1.0 \times 10^{-7}$, $N_{\rm O,dust}/N_{\rm H} = 154$ ppm (see text)				9.1 ± 0.6 [c]

[a] Asplund et al. (2009).
[b] Assuming $N(\rm H) + 2N(\rm H_2) = 10^{21.13 \pm 0.03}$ cm^{-2}.
[c] Assuming $N_{\rm O,dust}/N_{\rm H} = 154$ ppm.
[d] Cardelli et al. (1993).
[e] If $f(\text{C II]}2325\,\text{Å}) = 4.78 \times 10^{-8}$ (Morton 2003).
[f] If $f(\text{C II]}2325\,\text{Å}) = 1.00 \times 10^{-7}$ (see text).
[g] Savage et al. (1992).
[h] Morton (1975).
[i] Cardelli et al. (1994).
[j] Federman et al. (1993).
[k] Crinklaw et al. (1994).

2175 Å Feature

- Strong feature described by Drude profile.

$$C_{\mathrm{abs}} = \frac{\langle P \rangle}{\langle u \rangle c} = \frac{4\pi q^2}{mc} \frac{\gamma \omega^2}{(\omega - \omega_0)^2 (\omega + \omega_0)^2 + \gamma^2 \omega^2}$$
$$= \frac{4\pi q^2}{mc} \frac{\gamma}{\omega_0^2 \left(\frac{\omega}{\omega_0} - \frac{\omega_0}{\omega} \right)^2 + \gamma^2} .$$

- Central λ constant.
  - Width changes.
- Possibly inter-band transitions in carbon sheets.

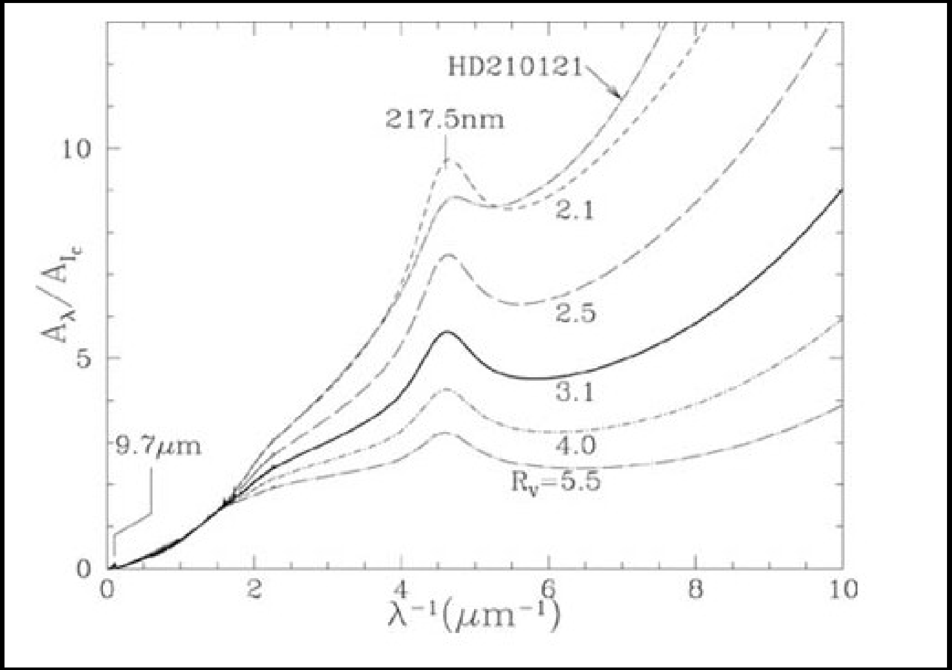

PAH Bands

- IR emission at 3.3, 62, 7.7, 8.6, 11.3, 12.7 μm from PAHs.

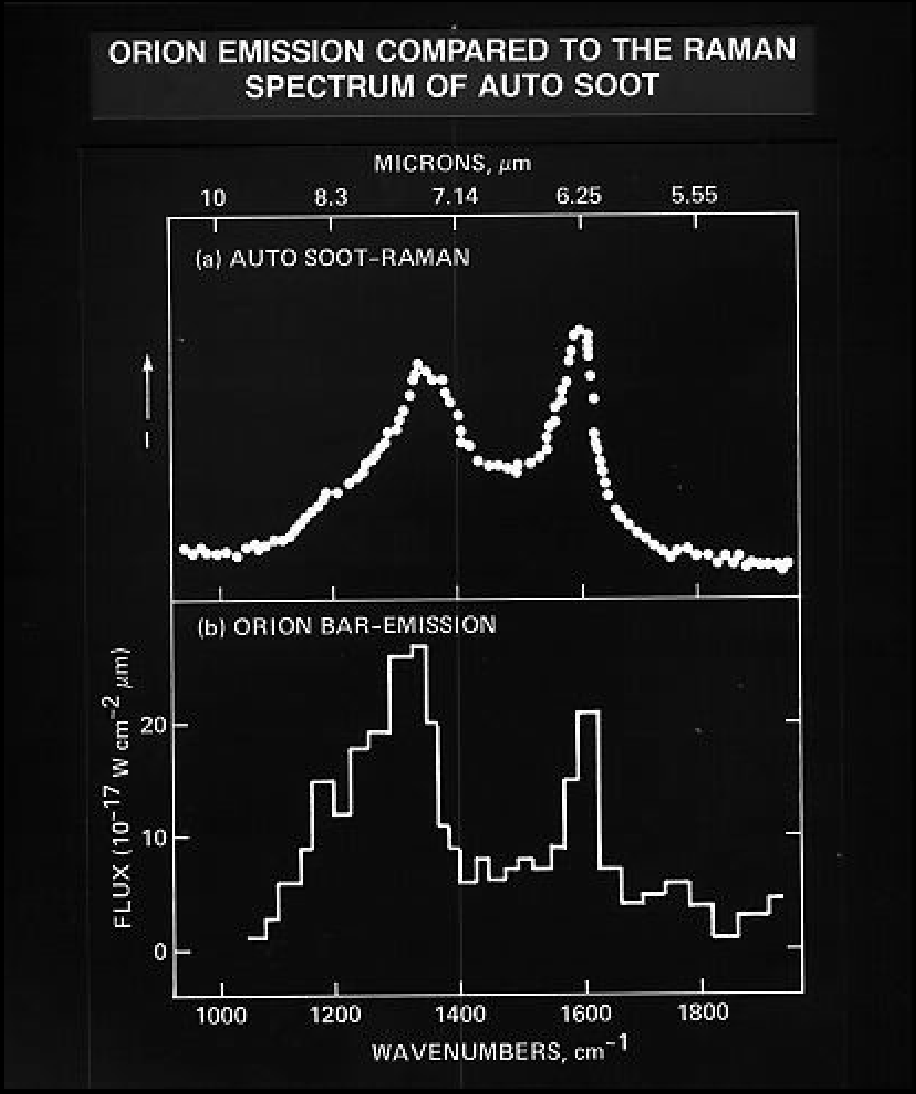

PAH Bands

- IR emission at 3.3, 62, 7.7, 8.6, 11.3, 12.7 μm from PAHs.
- Lines are from C-H bending and stretching modes.
- 15% of carbon in PAHs
- Thermal IR emission from stochastic heating of grains.

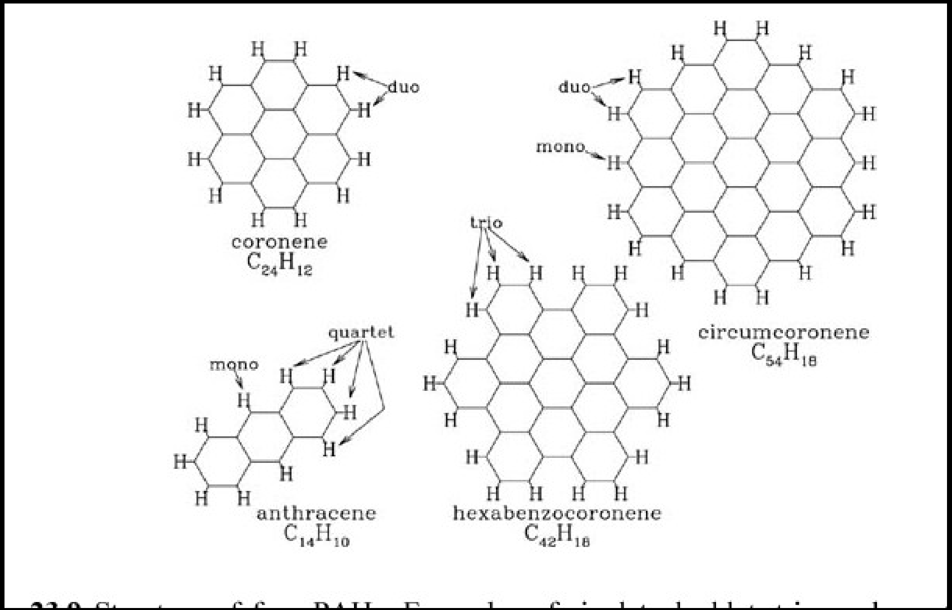

Silicates

- Absorption at 9.7 and 18 μm.
  - Silicate (SI-O) features.
- Profile is broad and smooth => amorphous.

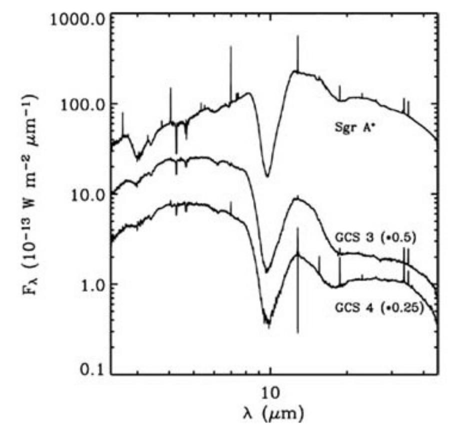

Figure 23.6 Spectra of the Galactic Center (Sgr A*), and two infrared sources GCS3 and GCS4 located near the Galactic Center. In all cases there is strong absorption in the 9.7 μm silicate feature, with associated weaker absorption in the 18 μm feature. There is also absorption in the 3.1 μm feature of H_2O ice toward Sgr A*, with weaker ice absorption seen toward GCS 3. From Kemper et al. (2004), reproduced by permission of the AAS.

Diffuse Interstellar Bands

- We don't talk about them.

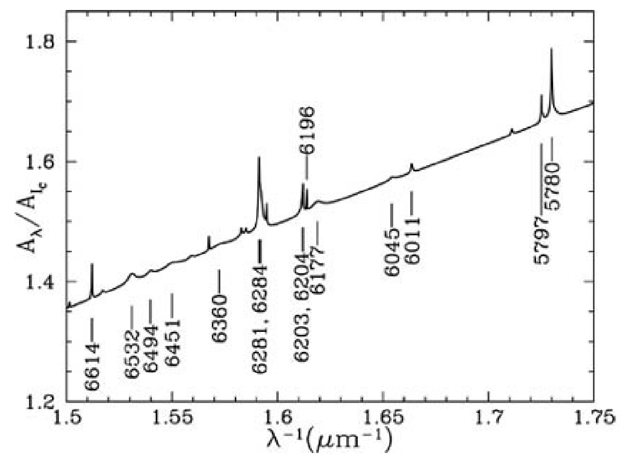

Figure 23.3 Extinction at wavelength λ (relative to the extinction at I_C = 8020 Å) for 6667 Å > λ > 5714 Å, showing some of the diffuse interstellar bands, based on the compilation by Jenniskens & Desert (1994).

Summary of Dust Composition

- Refractory elements are depleted onto dust.
  - Oxygen uncertain
- Carbon in the form of
  - graphite
  - diamond
  - PAHs
  - HACs.
  - SiC
  - Fullerenes
- Silicates.
- Ices in dark clouds.
  - Not in diffuse ISM.
- Thermal emission in IR.

Interstellar Dust Models

- MRN dust model
    - $dn/da \sim a^{-3.5}$
- Draine & Lee (1984)

- Amorphous silicates.
- Carbonaceous grains.
    - PAH-like for small grains.
    - Graphite-like for large grains.

Size Distribution

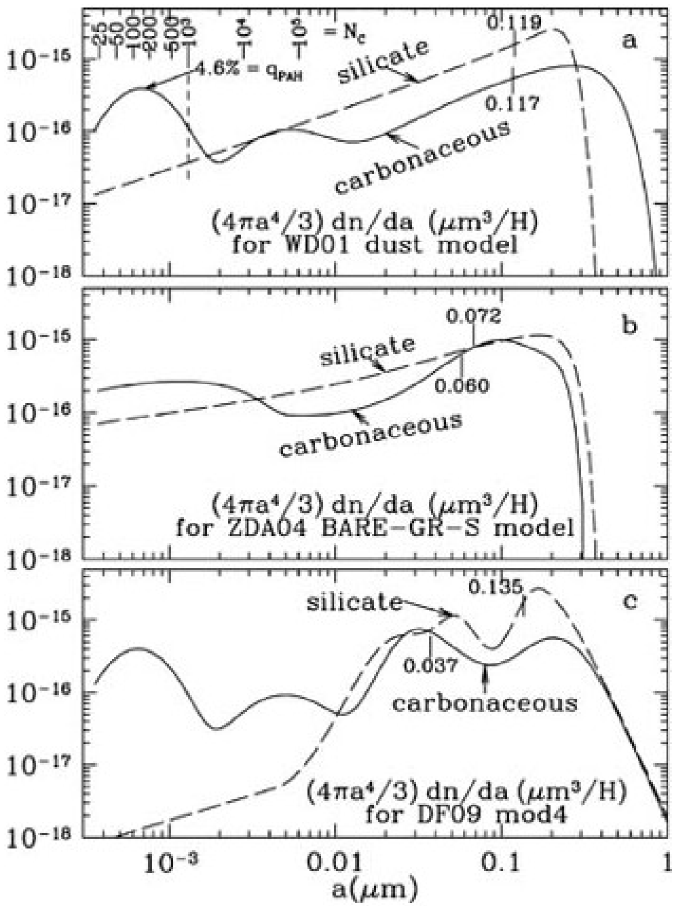

Figure 23.10 Size distributions for silicate and carbonaceous grains for dust models from (a) Weingartner & Draine (2001*a*), (b) Zubko et al. (2004), and (c) Draine & Fraisse (2009). The quantity plotted, $(4\pi a^3/3)dn/d\ln a$ is the grain volume per H per logarithmic interval in *a*. In each case, tick-marks indicate the "half-mass" radii for the silicate grains and carbonaceous grains.

Extinction Models

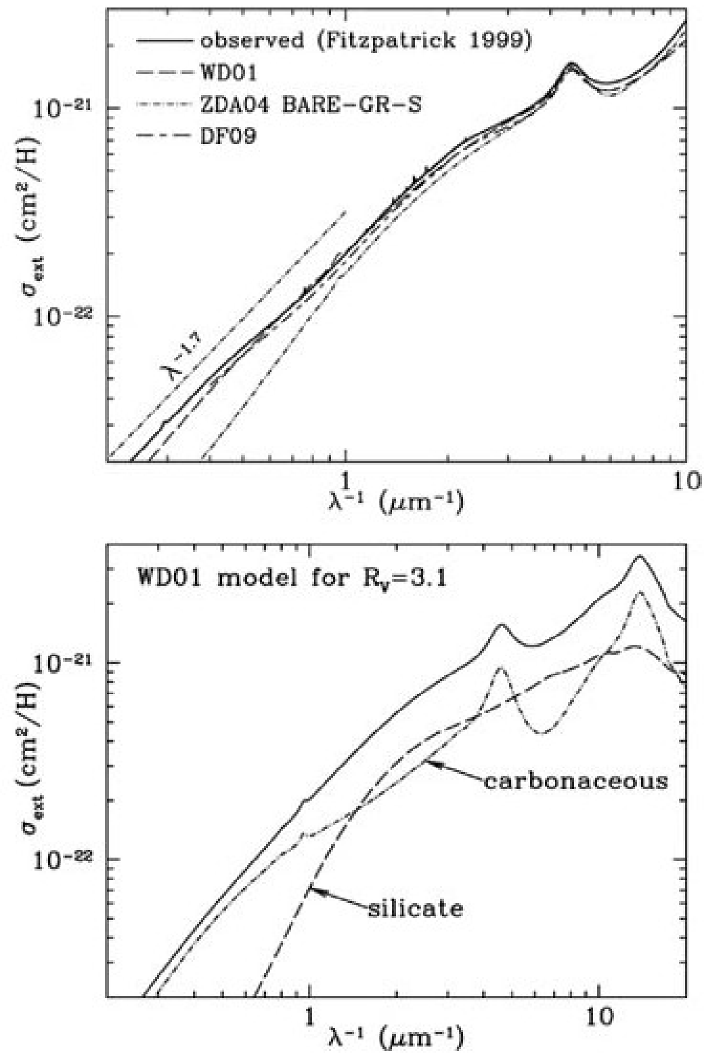

Figure 23.11 Upper: Average observed extinction for $R_V = 3.1$ (Fitzpatrick 1999) and extinction curves calculated for the WDO1 silicate-carbonaceous model (Weingartner & Draine 2001*a*) and for the ZDA04 BARE-GR-S silicate-carbonaceous model (Zubko et al. 2004). The WD01 model provides considerably more extinction in the infrared (1 to 4 μm) than the ZDA04 model (see text). Lower: Separate contributions of silicate and carbonaceous grains.

Dust Formation and Evolution

- Formed in outer atmospheres of post main sequence stars.
    - Shell from T ~ 1000 K out to end of stellar atmosphere.
    - Refractive elements condense onto grains.
    - Olivine, silicates.
    - Much of C, N, O locked up in the gas phase.

Dust Formation and Evolution

- Increase by coagulation.
- Gas molecules sticking to the surface.
- Grain growth encouraged in dense regions.
    - Icy mantles.
    - Surface organics.
- Evaporation in high radiation environments.
- Shock destruction of grains.

Temperatures

- Absorption or emission of photons.
- Inelastic collisions with grains/atoms/molecules.
- Large grains will absorb radiation and reradiate as heat.

- Classical (large) grains.
  - responsible for optical extintion.
- Small grains/large molecules.
  - FUV extinction.

Absorption by Dust

- Rate of heating:

$$\left(\frac{dE}{dt}\right)_{\rm abs} = \int \frac{u_\nu d\nu}{h\nu} \times c \times h\nu \times Q_{\rm abs}(\nu)\pi a^2$$

- number density x energy x cross-section

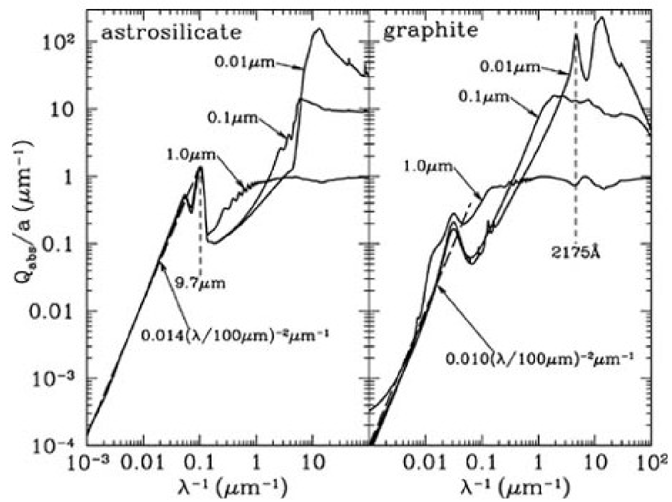

Figure 24.1 Absorption efficiency $Q_{\rm abs}(\lambda)$ divided by grain radius a for spheres of amorphous silicate (left) and graphite (right). Also shown are power-laws that provide a reasonable approximation to the opacity for $\lambda \gtrsim 20\ \mu$m.

Absorption by Dust

- Rate of heating:

$$\left(\frac{dE}{dt}\right)_{\rm abs} = \int \frac{u_\nu d\nu}{h\nu} \times c \times h\nu \times Q_{\rm abs}(\nu)\pi a^2$$

- number density x energy x cross-section
- Spectrum averaged cross-section.
    - Use MMP ISRF.
- $dE/dt = \langle Q_{abs} \rangle \pi a^2 uc$

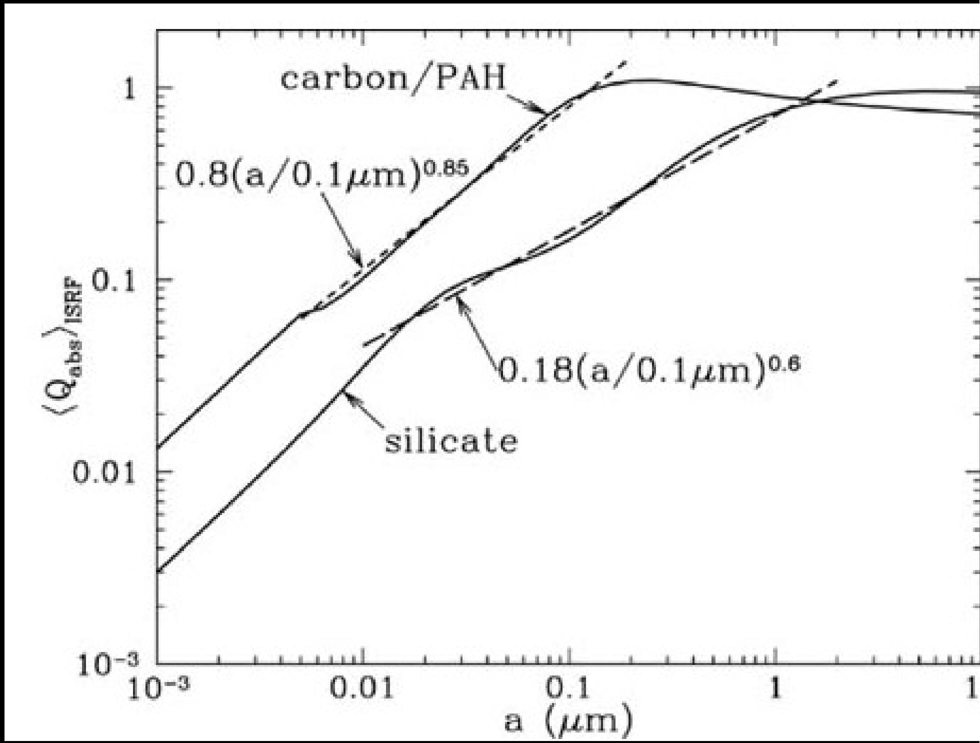

Collisional Heating

- Rate of heating:
- assuming Maxwellian velocities
- Mean speed:
- α: degree of inelasticity
- Collisional heating unimportant except in dark clouds.

$$\left(\frac{dE}{dt}\right)_{\text{gas}} = \sum_i n_i \left(\frac{8kT_{\text{gas}}}{\pi m_i}\right)^{1/2} \pi a^2 \times \alpha_i \times 2k(T_{\text{gas}} - T_{\text{dust}})$$

$$f(v) = \sqrt{\left(\frac{m}{2\pi kT}\right)^3} 4\pi v^2 \exp\left(\frac{-mv^2}{2kT}\right)$$

$$\langle v \rangle = \int_0^\infty v\, f(v)\, dv = \sqrt{\frac{8kT}{\pi m}} = \sqrt{\frac{8RT}{\pi M}} = \frac{2}{\sqrt{\pi}} v_p$$

Radiative Cooling

- Thermal emission in IR

$$\left(\frac{dE}{dt}\right)_{\text{emiss.}} = \int d\nu\, 4\pi B_\nu(T_d) C_{\text{abs}}(\nu) = 4\pi a^2 \langle Q_{\text{abs}}\rangle_{T_d} \sigma T_d^4\ ,$$

- Q correction factor for non-BB emission.

$$\langle Q_{\text{abs}}\rangle_T \equiv \frac{\int d\nu B_\nu(T) Q_{\text{abs}}(\nu)}{\int d\nu B_\nu(T)}$$

- In steady state:

$$4\pi a^2 \langle Q_{\text{abs}}\rangle_{T_{\text{ss}}} \sigma T_{\text{ss}}^4 = \pi a^2 \langle Q_{\text{abs}}\rangle_\star u_\star\, c$$

Radiative Cooling

- Thermal emission in IR
- Q correction factor for non-BB emission.
- In steady state:

$$4\pi a^2 \langle Q_{\rm abs}\rangle_{T_{\rm ss}} \sigma T_{\rm ss}^4 = \pi a^2 \langle Q_{\rm abs}\rangle_\star u_\star\, c$$

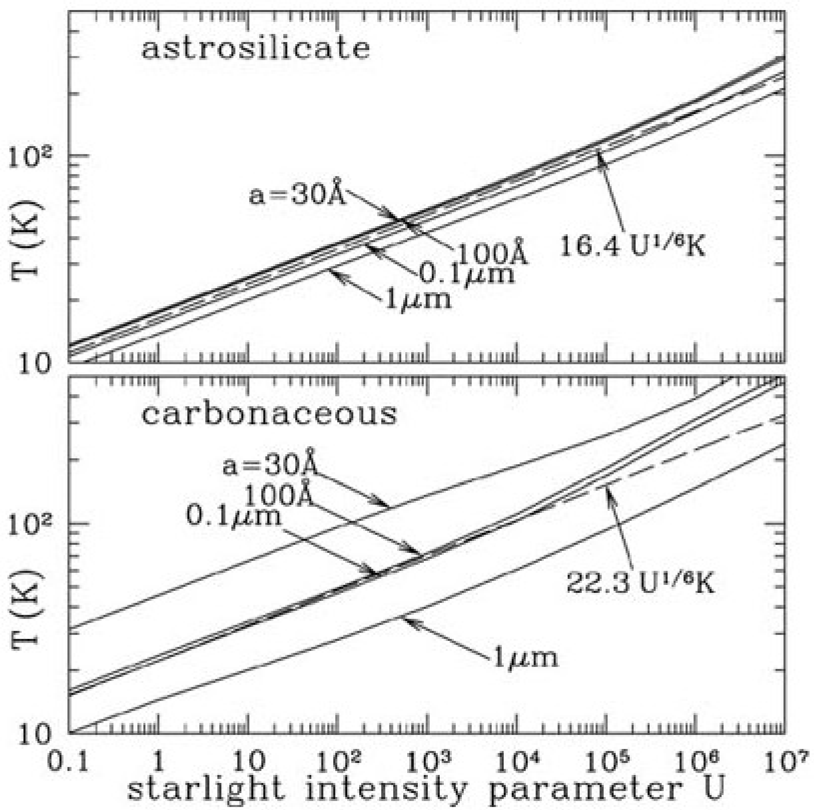

Figure 24.4 Equilibrium temperature for astrosilicate and carbonaceous grains heated by starlight with the spectrum of the local radiation field, and intensity U times the local intensity. Also shown are the power-laws $T = 16.4U^{1/6}$ K and $T = 22.3U^{1/6}$ for $a = 0.1$ μm from Eqs. (24.19 and 24.20).

Radiative Cooling

- Thermal emission in IR
- Q correction factor for non-BB emission.
- In steady state:

$$4\pi a^2 \langle Q_{\rm abs} \rangle_{T_{\rm ss}} \sigma T_{\rm ss}^4 = \pi a^2 \langle Q_{\rm abs} \rangle_{\star} u_{\star}\, c$$

- Stochastic heating from small grains.

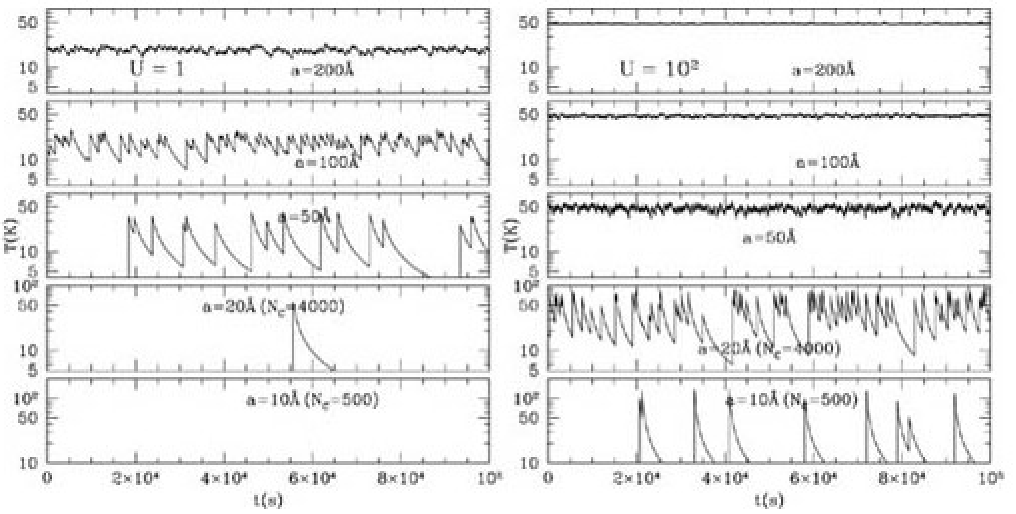

Figure 24.5 Temperature versus time during 10^5 s (Ø 1 day) for five carbonaceous grains in two radiation fields: the local starlight intensity (U = 1; left panel) and 10^2 times the local starlight intensity ($U = 10^2$; right panel). The importance of quantized stochastic heating is evident for the smaller sizes.

Thermal Emission from Grains

- 30% of starlight reradiated in IR.

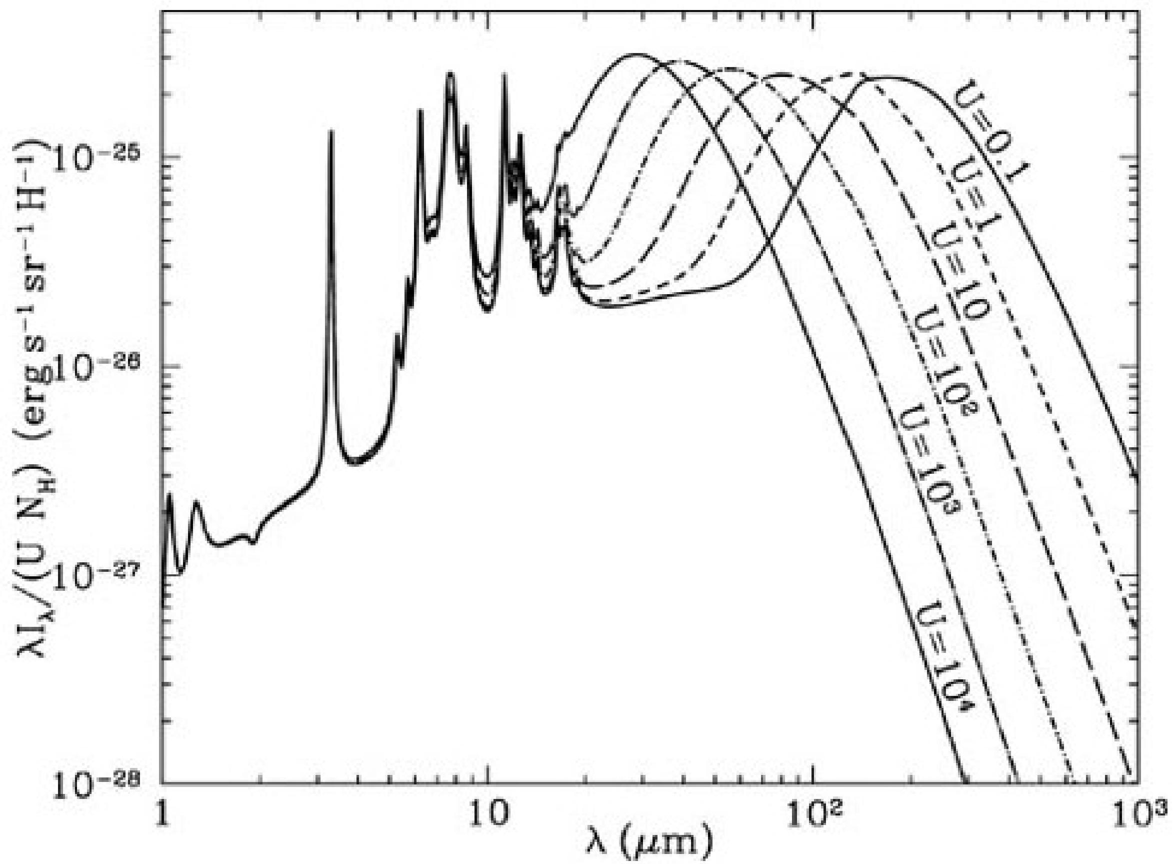

Figure 24.7 Infrared emission spectrum for model with silicate and graphite/PAH grains in ISRF intensity scale factor U from 0.1 to 10^4 ($U = 1$ is the local ISRF). Spectra are scaled to give power per H nucleon per unit U, calculated using the model of Draine & Li (2007).

Grain Charging

- Grains may be charged.
  - More collisions with electrons so negatively charged.
  - Photoionization drives grains to positive potentials.

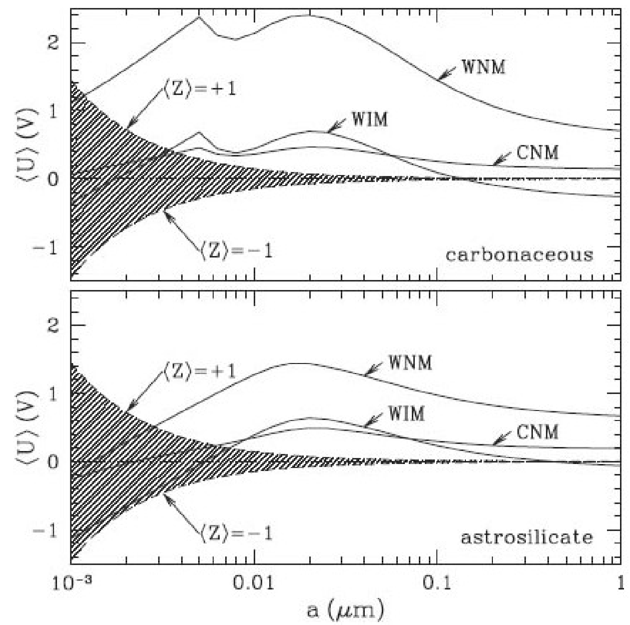

Figure 25.3 Time-averaged potential U as a function of grain size for silicate and carbonaceous grains for 3 different environments: CNM, WNM, and WIM. Also shown are potentials for $Z = \pm 1$; away from the (shaded) region bounded by these two curves, charge quantization is of secondary importance.